Changing Dynamical Complexity with Time Delay in Coupled Fiber Laser Oscillators

Anthony L. Franz,[1,2] Rajarshi Roy,[1,2,3] Leah B. Shaw,[4] and Ira B. Schwartz[4]
[1]*Department of Physics, University of Maryland, College Park, Maryland 20742, USA*
[2]*IREAP, University of Maryland, College Park, Maryland 20742, USA*
[3]*IPST, University of Maryland, College Park, Maryland 20742, USA*
[4]*Nonlinear Systems Dynamics Section, Plasma Physics Division, Code 6792, US Naval Research Laboratory, Washington, DC 20375, USA*
(Received 21 March 2007; published 2 August 2007)

We investigate the complexity of the dynamics of two mutually coupled systems with internal delays and vary the coupling delay over 4 orders of magnitude. Karhunen-Loève decomposition of spatiotemporal representations of fiber laser intensity data is performed to examine the eigenvalue spectrum and significant orthogonal modes. We compute the Shannon information from the eigenvalue spectra to quantify the dynamical complexity. A reduction in complexity occurs for short coupling delays while a logarithmic growth is observed as the coupling delay is increased.

DOI: 10.1103/PhysRevLett.99.053905 PACS numbers: 42.65.Sf, 05.45.Tp, 42.55.Wd

The dynamics of delay-coupled systems are rich and varied, and very important for the consideration of biological, chemical, and physical systems, including neurons, chemical reactions involving transport processes, laser systems, and electronic circuits [1,2]. Delays are often neglected for simplicity, and this may be a good approximation when they are very short compared to other system time scales. When this is not the case, as it has become very clear over the past decade, time delays play a very important role in the dynamics and function of networks of coupled elements, and they often influence their collective dynamics. The adaptive nature of systems with delays, such as the variability of the number of degrees of freedom involved at a given point in their time evolution, is of interest and significance for specific applications [3].

Studies of single time-delayed systems show that increasing delays typically lead to more complex, high dimensional dynamics [4]. We consider two systems with internal, fixed time delays that are mutually coupled with a second time delay that varies from well below to much above the internal delay. We use a spatiotemporal representation [5] that enables us to compactly view time series data for time scales spanning many orders of magnitude. The use of Karhunen-Loève (KL) decomposition techniques [6] then allows the data to reveal the number of orthogonal modes necessary for accurate reconstructions of the dynamics. KL decomposition has many broad applications including analyzing turbulence, performing face recognition, and examining transverse profiles of laser beams [7]. The KL modes form a basis that minimizes the entropy, or information, of the system as calculated from the eigenvalue spectrum [8]. We use the entropy as a quantitative measure of complexity [9] of the coupled-system dynamics and compute it as the coupling delay is varied. We find the interesting result that dynamical complexity reaches a minimum around the resonance delay condition for which the coupling delay is approximately equal to the internal delay.

As an illustration of these ideas we will examine the dynamics of two fiber lasers coupled with time delays that extend over 4 orders of magnitude. The experimental system of mutually delay-coupled erbium fiber lasers [10] is shown schematically in Fig. 1. The lasers were coupled with delay lines corresponding to a time of signal propagation of τ_d. The rings have closely matched cavity lengths with internal round-trip delay times for the light of $\tau_r = 213.9$ ns. The long cavity and broad gain bandwidth results in approximately 4000 lasing longitudinal modes in each uncoupled laser as calculated from optical spectra measurements and resonant cavity theory [11]. The active fiber in the two amplifiers is identically doped and matched in length to within 1 mm. The power in both rings was matched by adjusting the pumps, and the variable attenuators were used to match the power in the coupling lines. Both lasers were pumped at approximately 4.6 times the threshold value, and the coupling strength κ was adjusted with the variable attenuators to be 1.7% for these experiments. This means that the average light power injected into each ring from the other laser is 1.7% of the power internal to it. The coupling delay was varied between $\tau_d = 0.050$ μs and $\tau_d = 120$ μs by adding extra fiber to the coupling lines. Complete (identical) synchrony, which often appears with a time shift equal to τ_d, was observed

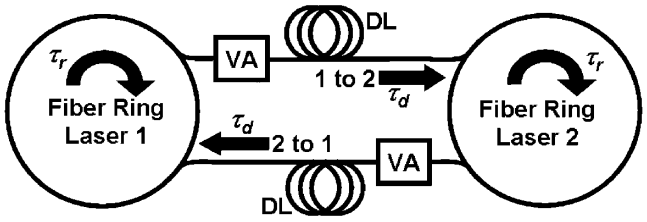

FIG. 1. Schematic of experimental apparatus. The arrows show the direction of light propagation through the rings and the coupling lines. DL, delay line (determines τ_d); VA, variable attenuator (adjusts κ).

for all our coupled measurements as confirmed by cross correlation synchronization analysis [12].

The lasers each have thousands of lasing modes that are nonlinear oscillators globally coupled through sharing population inversion. It is a daunting task to model the laser systems with hundreds or thousands of coupled-mode equations, since many unknown parameters relating to the mode coupling would be involved [13]. A time domain model that involves delay-differential equations has sometimes been employed as an alternative [2,14], but even this approach presents serious difficulties when long lengths of fiber with random birefringence fluctuations are involved. Because of these difficulties, typical of fiber laser systems, we chose to employ the KL decomposition of spatiotemporal representations of the time series data.

Since τ_r is constant for all of our observations, we associate discrete spatial positions, x_j, around the ring cavity with the discrete temporal measurements of intensity for each round-trip on the horizontal axis, normalized from 0 to 1. The intensity of the light at different positions around the ring is represented by a color coding scheme. The horizontal axis thus corresponds to a spatial view of the intensity of the laser light within the ring in one round-trip. Subsequent round-trips of data are indexed along the vertical axis. Since the temporal patterns do not change abruptly from round-trip to round-trip, but evolve over several trips, we choose every tenth round-trip for display. The round-trip number, n_t, denotes the evolution of the system dynamics.

In Figs. 2(a)–2(d) we provide four illustrative examples of spatiotemporal representations of experimental laser data in panels (I). These data, $u(x_j, n_t)$, are a discrete array with each point indexed by x_j and n_t that we will analyze with a KL decomposition [6]. First, for each value of x_j we subtract the mean for that position j averaged over all n_t. Next, we compute the covariance matrix, $\mathbf{K}$, with elements $K(x_j, x_{j'}) = \langle u(x_j, n_t)u(x_{j'}, n_t)\rangle$, where the angle brackets refer to time averaging. Then we calculate the eigenvalues $\tilde{\lambda}_i$ and eigenvectors $\psi_i(x_j)$ of $\mathbf{K}$. The $\psi_i(x_j)$ are orthogonal KL modes that describe a spatial pattern of the intensity over a round-trip. A sampling of these are shown in panels (II) for each set of figures. The original data can be written in terms of an expansion

$$u(x_j, n_t) = \sum_{i=1}^{N} \alpha_i(n_t)\psi_i(x_j) \qquad (1)$$

that uses the KL modes as its basis, where N is the number of modes. Each mode has a coefficient, $\alpha_i(n_t)$, that weights the impact of that mode on the round-trip pattern at round-trip n_t. Panels (III) show the $\alpha_i(n_t)$ corresponding to the $\psi_i(x_j)$ in panels (II). The coefficients as a function of time are calculated with $\alpha_i(n_t) = \sum_j u(x_j, n_t)\psi_i(x_j)$ where $\langle \alpha_i(n_t)\alpha_k(n_t)\rangle = \tilde{\lambda}_i\delta_{ik}$. $\tilde{\lambda}_i$ is the eigenvalue corresponding to KL mode i and δ_{ik} is the Kronecker delta function. The modes with the largest eigenvalues will be the most important in the expansion of Eq. (1) so we order the eigenvalues from largest, $\tilde{\lambda}_1$, to smallest, $\tilde{\lambda}_N$, and normalize them by the sum of all the eigenvalues. Panels (IV) show the 25 largest normalized eigenvalues, λ_i, on a logarithmic scale.

The typical dynamics of a single uncoupled fiber laser is shown in Fig. 2(a) panel (I). The spatial patterns for the intensity in each round-trip change slowly with time, as shown by the time evolution of the mode coefficients in panel (III). The eigenvalue spectrum in panel (IV) shows an initial fast decay and then a slower tail.

Figure 2(b) is for the minimum value of coupling delay of 50 ns. The mutual coupling induces a substantial narrowing of each laser's optical spectra and a strongly periodic intensity oscillation in each ring, even though the uncoupled fiber lasers are aperiodic in their dynamics. The periodicity of the oscillations is slightly incommensurate with the round-trip time, and eventually the pattern switches to a different one, after about 3000 round-trips. The two strongest spatial modes are shown in panel (II), as is the 10th mode. Panel (III) shows the coefficients for these three modes and reveals that the first two modes are dominant in representing the dynamical evolution of the laser, with much smaller contributions from the tenth. The eigenvalue spectrum in panel (IV) shows a fast exponential decay over 4 orders of magnitude, with a much slower decay thereafter.

Figure 2(c) is for $\tau_d = 218$ ns that has deliberately been adjusted to match the round-trip time internal delay of each fiber ring, which is the resonant delay condition. In this case, we see the regular periodicity of Fig. 2(b) replaced by a much different temporal pattern. There is no clear periodicity in the KL modes on the time scale of one round-trip, and the pattern evolves continuously over the entire time of observation. Interestingly, a very small number of modes once again can represent the dynamical evolution with good accuracy, and the eigenvalue spectrum decays in a way quite similar to that of Fig. 2(b).

Figure 2(d) shows a result typical of very long coupling delays, in this case illustrated for $\tau_d = 120$ μs. The spatiotemporal pattern is now vastly different from the three other ones. The round-trip pattern changes over only a few round-trips, and now the dominant period observed is $2\tau_d$, over the entire measurement. Even though the KL mode coefficients do decrease in strength, many more modes are now necessary to represent the dynamical evolution accurately, and the mode coefficients remain comparable in magnitude. The eigenvalue spectrum still decays exponentially, but at a significantly slower rate than in Figs. 2(b) and 2(c), and over only 1 order of magnitude for the first 25 eigenvalues.

The major conclusion of our experiments is shown in Fig. 3. While inspecting the number of significant KL modes involved in the dynamics provides a simple reckoning of the dynamical complexity, it is preferable to use a

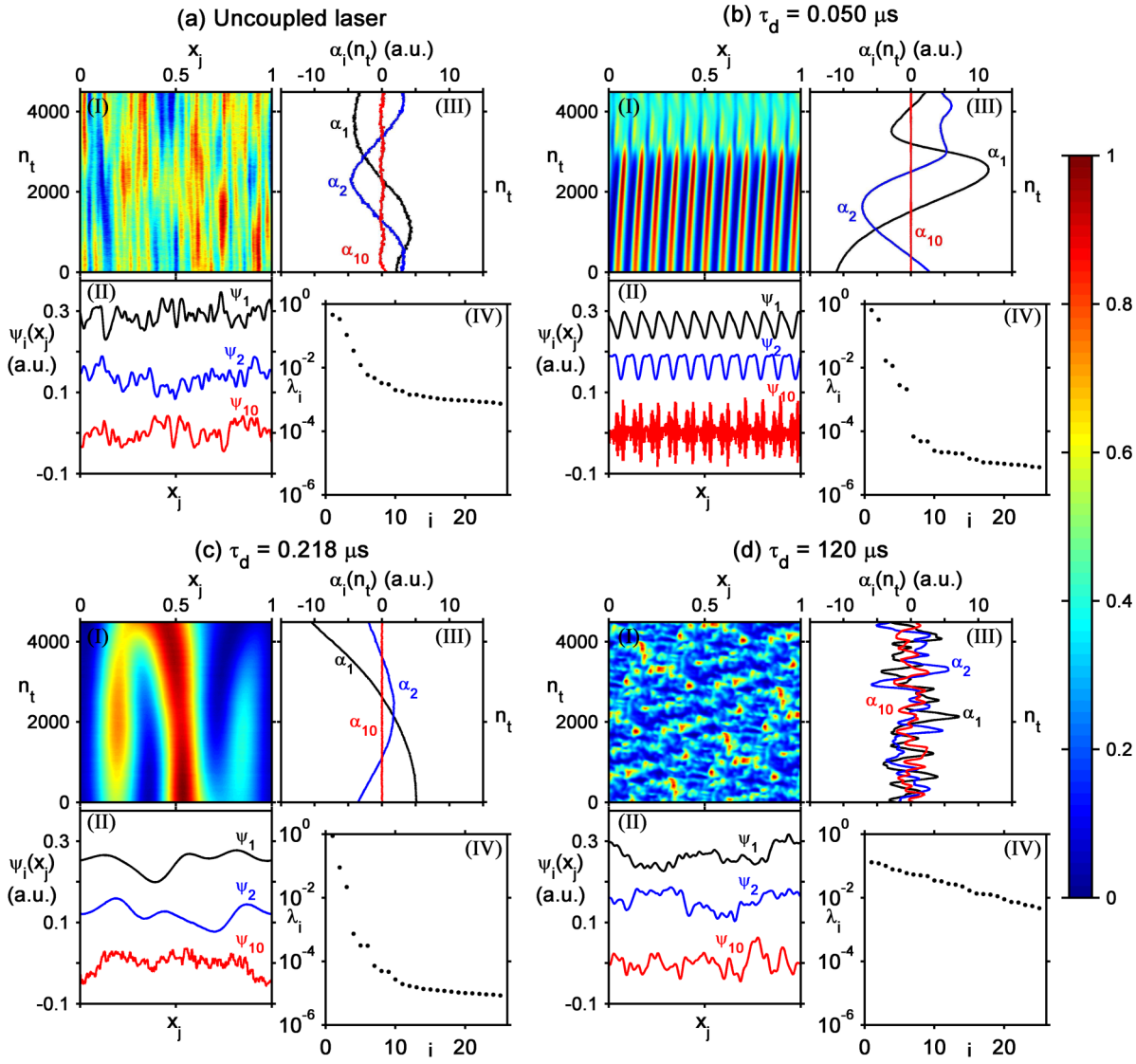

FIG. 2 (color online). (a) KL decomposition for an uncoupled laser. KL decompositions for mutually coupled lasers with (b) $\tau_d = 0.050$ μs, (c) $\tau_d = 0.218$ μs, and (d) $\tau_d = 120$ μs. For (a)–(d) panel (I) is the spatiotemporal representation of the intensity dynamics, panel (II) shows some KL modes $\psi_i(x)$ associated with eigenvalues λ_i (modes above the bottom mode are offset for clarity), panel (III) shows the corresponding expansion coefficients, $\alpha_i(n_t)$, for the KL modes in (II), and panel (IV) shows the 25 largest normalized eigenvalues, λ_i, on a logarithmic scale. The bar to the right maps the colors in panels (I) to normalized intensity values.

measure that quantitatively utilizes the eigenvalue spectrum for this purpose. Here we have used a connection between an information measure and the KL decomposition to quantitatively highlight the change in complexity of the mutually coupled-system dynamics.

The relationship between Shannon's entropy (or information) [15] and the KL decomposition is made by interpreting the normalized eigenvalues λ_i of the covariance matrix, $\mathbf{K}$, as the probabilities P_i to find the system in state i [6,8] so that

$$H = -\sum_i P_i \log_2 P_i = -\sum_i \lambda_i \log_2 \lambda_i. \qquad (2)$$

The entropy, H, then provides a measure of the distribution or rate of decay of the magnitude of the ordered eigenvalues. This leads us to a quantitative assessment of the complexity of the system dynamics, as shown in Fig. 3.

The spatiotemporal representations for the uncoupled lasers show more complexity or higher information content than for the systems coupled with short delays, and the information content is about 2 to 2.5 bits. The information in the spatiotemporal representations cannot be compressed as easily as for the case with the periodic dynamics in Fig. 2(b), or even in Fig. 2(c), which contain progressively smaller amounts of information per pixel of the figures. In an extreme case, if there were only one domi-

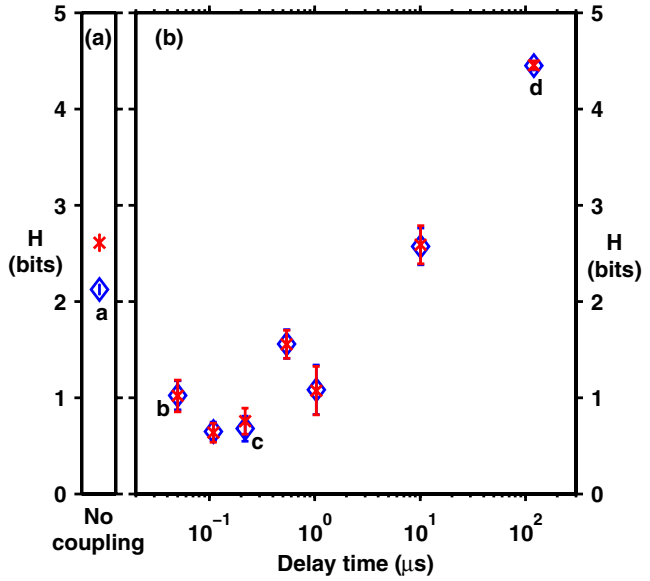

FIG. 3 (color online). (a) Entropy H, for the uncoupled lasers. (b) Entropy H, for the lasers coupled with different delays, τ_d. Blue ◇: laser 1, red X: laser 2. The error bars in both plots are the statistical standard error based on a sample set of ten. The letters by four data points identify the set of panels in Fig. 2 that displays one of the time series represented by that point.

nant eigenvalue, then the information could be represented by only one spatial mode or coordinate, and H reaches its minimum, zero. In our case, the minimum value is about 0.6 bits per pixel, reached when $\tau_d = 0.109$ μs or when $\tau_d \approx \tau_r$. As the τ_d is increased from this point, we see that the complexity or information content of the dynamics increases as well, roughly as the logarithm of the delay time. In Fig. 2(d) the information content is about 4.5 bits per pixel. For comparison we generated several 2D images of uniformly distributed random numbers. The images had the same number of pixels as our spatiotemporal representations, and the average value of H is approximately 8 bits per pixel.

Our results demonstrate that varying the coupling delay can result in a nonmonotonic change of complexity of the dynamics as measured by the Shannon information derived from the KL eigenvalue spectrum. Our analysis suggests that highly regular periodic oscillations with frequencies close to multiples of the fundamental internal frequency, and a decrease in the number of effective degrees of freedom of the system, result when fiber laser oscillators with slightly different parameters are coupled with short delays. When the coupling delay is increased beyond the coherence time of the individual oscillators, we obtain irregular waveforms with much longer periodicity and increasing complexity. For small τ_d the differences between the two lasers constrain and reduce the dynamics to a smaller common set of modes. For very long τ_d, patterns are stored in the delay lines and contribute to the increasing complexity. Further measurements at delays near $\tau_d = \tau_r$ are necessary to clarify details of the complexity minimum.

We gratefully acknowledge support from the Office of Naval Research and the US Air Force Center for Array Analysis. A. L. F. acknowledges support from the Air Force Institute of Technology. L. B. S. is supported by a National Research Council Research Associateship. We thank Professor Prakash Narayan and Dr. Beth Dakin for many helpful discussions.

[1] M. C. Mackey and L. Glass, Science **197**, 287 (1977); R. Holz and F. W. Schneider, J. Phys. Chem. **97**, 12 239 (1993); M. Kim *et al.*, Science **292**, 1357 (2001); R. Lang and K. Kobayashi, IEEE J. Quantum Electron. **16**, 347 (1980); D. V. Ramana Reddy, A. Sen, and G. L. Johnston, Phys. Rev. Lett. **85**, 3381 (2000).
[2] K. Ikeda, Opt. Commun. **30**, 257 (1979).
[3] H. G. Schuster, *Complex Adaptive Systems* (Scator Verlag, Saarbrücken, Germany, 2001).
[4] J. D. Farmer, Physica (Amsterdam) **4D**, 366 (1982).
[5] F. T. Arecchi *et al.*, Phys. Rev. A **45**, R4225 (1992); G. Giacomelli and A. Politi, Phys. Rev. Lett. **76**, 2686 (1996); M. J. Bünner *et al.*, Eur. Phys. J. D **10**, 165 (2000); **10**, 177 (2000).
[6] M. Kirby, *Geometric Data Analysis* (Wiley, New York, 2001).
[7] L. Sirovich, Q. Appl. Math. **XLV**, 561 (1987); L. Sirovich and M. Kirby, J. Opt. Soc. Am. A **4**, 519 (1987); O. Hess, Chaos, Solitons & Fractals **4**, 1597 (1994).
[8] S. Watanabe, *Transactions of the Fourth Prague Conference on Information Theory, Statistical Decision Functions and Random Processes, 1965* (Academia, Prague, 1967), pp. 635–660.
[9] For measures of complexity, see R. Badii and A. Politi, *Complexity* (Cambridge University Press, Cambridge, England, 1997).
[10] E. A. Rogers-Dakin *et al.*, Phys. Rev. E **73**, 045201(R) (2006).
[11] A. E. Siegman, *Lasers* (University Science Books, Sausalito, CA, 1986), Chap. 11.
[12] L. B. Shaw *et al.*, Chaos **16**, 015111 (2006).
[13] E. Desurvire, in *Rare-Earth-Doped Fiber Lasers and Amplifiers*, edited by M. J. F. Digonnet (Marcel Dekker, New York, 2001), 2nd ed.
[14] Q. L. Williams, J. García-Ojalvo, and R. Roy, Phys. Rev. A **55**, 2376 (1997).
[15] T. M. Cover and J. A. Thomas, *Elements of Information Theory* (Wiley, New York, 2006), Chap. 2, 2nd ed.